$^{13}C(\vec{p},p')^{13}C^*$ reaction at $T_p = 547$ MeV

S. J. Seestrom-Morris, M. A. Franey, D. Dehnhard, and D. B. Holtkamp*
University of Minnesota, Minneapolis, Minnesota 55455

R. L. Boudrie, J. F. Amann, and G. C. Idzorek
Los Alamos National Laboratory, Los Alamos, New Mexico 87545

C. A. Goulding*
University of Texas, Austin, Texas 78712
(Received 21 February 1984)

Differential cross sections and analyzing powers have been measured between $\theta_{lab} = 6.5°$ and 34.5° for scattering of 547-MeV polarized protons from ^{13}C. Data for the $\frac{1}{2}^-$ (0.0), $\frac{1}{2}^+$ (3.09), $\frac{3}{2}^-$ (3.68), $\frac{5}{2}^+_1$ (3.85), $\frac{5}{2}^+_2$ (6.86), $\frac{5}{2}^-$ (7.55), $\frac{1}{2}^-_2$ (8.86), and $\frac{9}{2}^+$ (9.50) states are presented. The elastic scattering data were analyzed with a potential calculated in the impulse approximation and the resulting distorted waves were used in the distorted-wave impulse approximation analysis of the inelastic data with microscopic transition densities based on shell model wave functions.

I. INTRODUCTION

In a recent study[1] of inelastic pion scattering from ^{13}C, several transitions were found to be well described by distorted wave impulse approximation (DWIA) calculations[2] using microscopic transition densities[2-4] derived from shell-model calculations. For other transitions, however, these calculations failed to describe the data. Since these discrepancies might be due to either deficiencies in the reaction model or in the nuclear structure calculations, it is important to investigate the same transitions with other probes. We have therefore measured with polarized protons of incident energy $T_p = 547$ MeV cross sections and analyzing powers for elastic scattering from ^{13}C and for the transitions to the states of $J^\pi(E_x) = \frac{1}{2}^+$ (3.09 MeV), $\frac{3}{2}^-$ (3.68 MeV), $\frac{5}{2}^+$ (3.85 MeV), $\frac{5}{2}^+$ (6.86 MeV), $\frac{5}{2}^-$ (7.55 MeV), $\frac{1}{2}^-_2$ (8.86 MeV), and $\frac{9}{2}^+$ (9.50 MeV).

Medium energy inelastic proton scattering from ^{13}C has been studied before at $T_p = 135$ (Refs. 5 and 6) and 800 MeV (Refs. 7 and 8). Proton scattering at 500 MeV offers several advantages over both the lower and higher energy experiments. At 500 MeV the impulse approximation (IA) is expected to be more valid than at 135 MeV; the free nucleon-nucleon (NN) interaction, particularly the proton-neutron force, is better determined than at 800 MeV; and the relative strength of the spin-dependent interaction (compared to the spin-independent interaction) is larger than at both of these other energies.

We have analyzed our data by DWIA calculations using the one-body density matrix elements of Cohen and Kurath[2,3] for the negative-parity states and those of Millener and Kurath[4] for the positive-parity states. An updated version[9] of the effective NN interaction of Ref. 10 was used in the DWIA calculations. The results of our analysis are completely consistent with those from pion scattering.[1,2]

II. EXPERIMENT

The high resolution spectrometer (HRS) at the Clinton P. Anderson Meson Physics Facility was used to measure differential cross sections and analyzing powers for 547-MeV polarized proton scattering from ^{13}C between $\theta_{lab} = 6.5°$ and 34.5° in 2° steps. The particle detection system consisted of the standard HRS focal plane delay-line readout drift chambers and trigger scintillators. Details of this setup have been reported elsewhere.[11] The overall energy resolution depended on the scattering angle and varied from 100 to 150 keV (FWHM). A typical energy spectrum at $\theta_{lab} = 16.5°$ is shown in Fig. 1.

The beam polarization P_b was reversed at the polarized ion source with a cycle time of 3 min, and logic levels generated at the source were used to identify each event according to the direction of P_b (i.e., up or down with respect to the scattering plane). The beam polarization

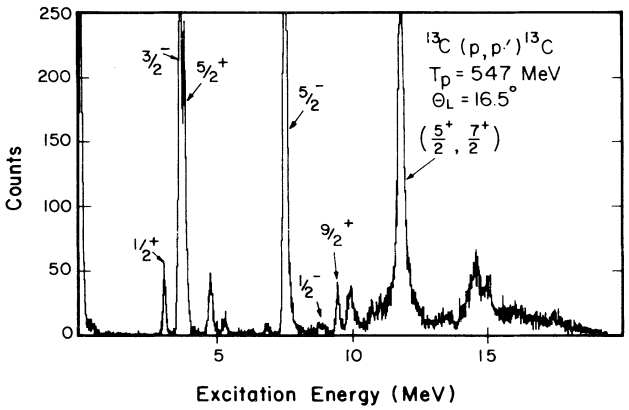

FIG. 1. Energy spectrum from $^{13}C(\vec{p},p')$ at $T_p = 547$ MeV and $\theta_{lab} = 16.5°$. Spin orientation direction is up.

was continuously monitored during data acquisition using a hydrogen polarimeter located about 10 m upstream of the target. The value of P_b was calculated from ratios of scaler counts in the left and right arms of the polarimeter for spin up and spin down. These ratios are designed to cancel any first-order geometrical false asymmetries in the polarimeter.

The target was a carbon wafer of areal density 50 mg/cm^2, enriched in ^{13}C to 96%. Absolute normalizations were obtained by measuring yields for p + p scattering from a CH_2 target of areal density 65 mg/cm^2 at $\theta_{lab}=24.5°$, 26.5°, and 32.5° and comparing them to cross sections from the phase shift solution WI82 of Arndt.[12]

Scattering angles were calculated to an accuracy of 0.10° for each event using the information derived from the drift chambers. This made it possible to separate the full angular acceptance of the spectrometer ($\simeq 2°$) into five angle bins of 0.35° angular width each. Peak areas were extracted from the spectra for each angle bin and beam polarization direction. For all groups, except the $\frac{3}{2}^-, \frac{5}{2}^+$ (3.68,3.85 MeV) doublet, counts above a linear background were summed. For the doublet, separate areas were extracted for the two states using the fitting option of the code PEKFIT.[13] Consistency checks were made by refitting some spectra with the lineshape oriented fitting code LOAF.[14] Analyzing powers were calculated for each state and angle bin using the equation

$$A_y=\frac{1}{P_b}\frac{(\sigma\uparrow-\sigma\downarrow)}{(\sigma\uparrow+\sigma\downarrow)}, \tag{1}$$

where $\sigma\uparrow$ and $\sigma\downarrow$ are the spin-up and spin-down yields. For the weak transitions to the $\frac{1}{2}^+$, $\frac{5}{2}_1^+$, $\frac{5}{2}_2^+$, $\frac{1}{2}_2^-$, and $\frac{9}{2}^+$ states the A_y data were averaged over three, or in some cases, five adjacent angular bins to reduce the statistical errors. The $\frac{9}{2}^+$-state cross section, which varies slowly with angle, was also averaged. The experimental data are present in Sec. III A and Sec. III B together with the results of the DWIA analysis.

The error bars plotted with the cross section and analyzing power data represent statistical uncertainties only, except for the 3.85/3.68 doublet. For that case an additional 10% uncertainty was included to account for additional uncertainties introduced by the peak fitting of the doublet. Uncertainties of 15% in the hydrogen normalization, 3% in chamber efficiency correction, and 3% in computer live time correction result in an overall systematic uncertainty of 16%.

III. ANALYSIS

A. Elastic scattering

The inelastic scattering program DWBA70 (Ref. 15) was modified to calculate elastic scattering observables using relativistic kinematics (described in Ref. 8) and an optical potential obtained in the impulse approximation (IA). The spin-independent and spin-orbit potentials were generated by folding[16] an updated version[9] of the $T_p=515$ MeV t matrix of Ref. 10 with the point proton and neutron densities, RHOX, of Ref. 17. This version of the NN interaction was derived from a more recent set of NN scattering amplitudes and differs little from the older one in its predictions of the observables measured in our experiment.

Data and predictions (solid lines) for the elastic differential cross sections $\sigma(\theta)$ and analyzing powers $A_y(\theta)$ are presented in Fig. 2. The angular distribution is well described at low momentum transfer, q, up to the first minimum near $q=1.4$ fm^{-1} and at the second maximum near $q=1.8$ fm^{-1}, but the calculated minima are deeper than those of the data. The qualitative features of the elastic $A_y(\theta)$ are also well represented by the IA predictions. In particular, the large negative value ($A_y\simeq-0.6$) near $q=1.4$ fm^{-1} is reproduced, although the calculated positive maxima are too large. The presence of a deep forward-angle dip in $A_y(\theta)$ at a momentum transfer near the first minimum in $\sigma(\theta)$ is a common feature of elastic data[18] at this bombarding energy. However, the IA does

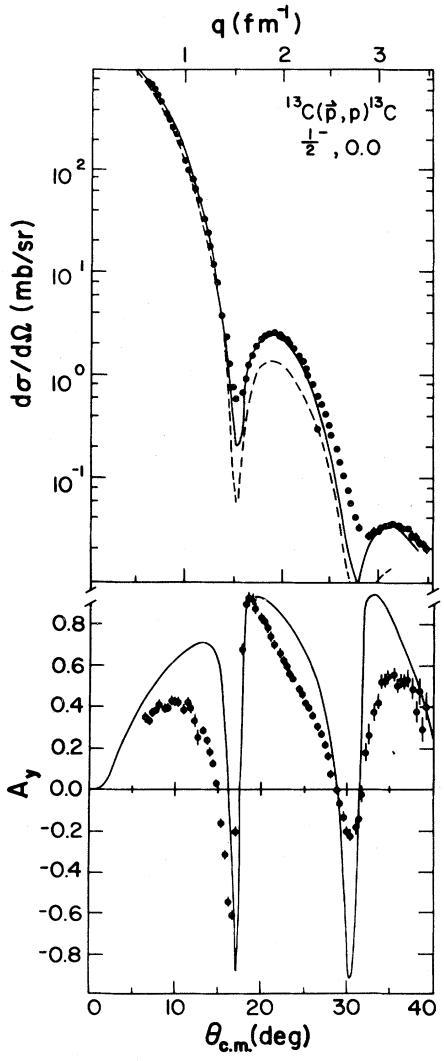

FIG. 2. Differential cross sections $d\sigma/d\Omega_{c.m.}$ and analyzing powers A_y for elastic scattering of 547 MeV protons from ^{13}C. Solid curves: IA calculations with the ground state densities derived from pion scattering (Ref. 17). Dashed curves: the same calculations without the spin-orbit force.

TABLE I. One body density matrix elements for negative parity states in ^{13}C. The OBDME are as defined in Refs. 2 and 4. The Z coefficients used with DWBA70 are obtained by multiplying these by $[(2J_f+1)/(2J_i+1)(2J+1)]^{1/2}$. $p3$ and $p1$ on the left-hand side indicate a "particle" in the $1p_{3/2}$ and $1p_{1/2}$ orbitals, respectively. $p3$ and $p1$ on the right-hand side indicate a "hole" in the $1p_{3/2}$ and $1p_{1/2}$ shells, respectively.

J_f^π	E_{exp}	J	P/N	$(p3p3)$	$(p3p1)$	$(p1p3)$	$(p1p1)$
$\frac{1}{2}^-_2$	8.86	1	N	−0.039	+0.022	−0.002	−0.086
			P	+0.063	+0.303	+0.774	+0.010
		0	N	−0.043	0.	0.	+0.060
			P	−0.087	0.	0.	+0.123
$\frac{3}{2}^-$	3.68	1	N	−0.068	+0.132	−0.579	−0.0004
			P	+0.056	+0.013	−0.006	+0.036
		2	N	−0.038	+0.033	+0.748	0.
			P	−0.159	−0.336	+0.594	0.
$\frac{5}{2}^-$	7.55	2	N	−0.052	−0.220	−0.0005	0.
			P	−0.130	−0.278	+0.790	0.

not reproduce[18] this dip for nuclei heavier than $A\simeq 16$. For ^{16}O, at $T_p=500$ MeV, the dip in the predicted $A_y(\theta)$ is located at the correct momentum transfer, but it is not deep enough to reproduce the data.[19]

B. Inelastic scattering

1. General remarks

The inelastic data were analyzed by microscopic DWIA calculations performed with a modified version of the code DWBA70.[15] The interaction used in the inelastic calculations was the same as described in Sec. III A. The zero-range approximation of Ref. 10 was used to calculate the knockon exchange terms for the central and spin-orbit interactions, but an exact calculation of the exchange was done for the tensor interaction. The entrance and exit channel distorted waves employed in the inelastic calculations were generated via the same optical potentials from which the elastic scattering observables (Sec. III A) were obtained.

TABLE II. One body density matrix elements for positive parity states in ^{13}C. The OBDME are as defined in Refs. 2 and 4. The Z coefficients used with DWBA70 are obtained by multiplying these by $[(2J_f+1)/(2J_i+1)(2J+1)]^{1/2}$. $d5$, $d3$, and $s1$ on the left-hand side indicate a "particle" in the $1d_{5/2}$, $1d_{3/2}$, and $2s_{1/2}$ orbitals, respectively. $p3$ and $p1$ on the right-hand side indicate a "hole" in the $1p_{3/2}$ and $1p_{1/2}$ orbitals, respectively.

J_f^π	E_{exp}	J	P/N	$(d5p3)$	$(d5p1)$	$(d3p3)$	$(d3p1)$	$(s1p3)$	$(s1p1)$
$\frac{1}{2}^+$	3.09	1	N	−0.238	0.	−0.004	−0.005	+0.057	+0.944
			P	−0.078	0.	+0.016	−0.008	+0.081	+0.010
		0	N	0.	0.	+0.037	0.	0.	+0.547
			P	0.	0.	−0.003	0.	0.	+0.004
$\frac{5}{2}^+_1$	3.85	2	N	−0.195	−0.655	−0.074	+0.002	−0.090	0.
			P	+0.008	−0.002	+0.002	+0.0003	+0.0003	0.
		3	N	+0.066	−0.788	+0.100	0.	0.	0.
			P	−0.089	−0.020	+0.069	0.	0.	0.
$\frac{5}{2}^+_2$	6.86	2	N	−0.245	+0.037	−0.008	+0.004	+0.554	0.
			P	+0.018	+0.005	−0.010	+0.003	−0.022	0.
		3	N	+0.143	+0.029	+0.030	0.	0.	0.
			P	−0.016	−0.021	+0.033	0.	0.	0.
$\frac{9}{2}^+$	9.50	4	N	0.635	0.	0.	0.	0.	0.
			P	0.001	0.	0.	0.	0.	0.

The one-body density matrix elements (OBDME) needed to calculate the microscopic transition densities were the same as previously used by Lee and Kurath[2] in their calculation of pion inelastic scattering. These have been derived[2] from the $1p$-shell wave functions of Cohen and Kurath[3] (CK) for the negative-parity states and from the $1p$-$2s$ $1d$ shell wave functions of Millener and Kurath[4] (MK) for the positive-parity states. Tables I and II list the OBDME of CK and MK in the jj representation. The radial dependences of the transition densities for all states were calculated with harmonic oscillator wave functions using the same oscillator parameter as Ref. 2, $b=1.67$ fm.

Additional microscopic transition densities were obtained by scaling the CK and MK one-body density matrix elements using effective charges. The effective charges were adjusted to obtain agreement with the absolute cross sections for the $\frac{3}{2}^-$, $\frac{5}{2}^-$, and $\frac{5}{2}_1^+$ states.

2. *Transition to the $\frac{1}{2}^+$ (3.09 MeV) state*

The data for the $\frac{1}{2}^+$ state at 3.09 MeV are shown in Fig. 3 together with the results of the DWIA calculations.

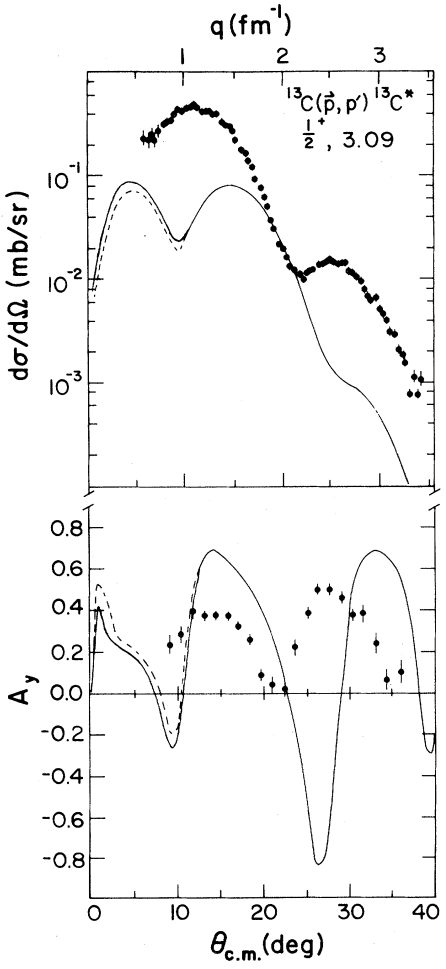

FIG. 3. $d\sigma/d\Omega_{c.m.}$ and A_y for the transition to the $\frac{1}{2}^+$ (3.09 MeV) state. Solid curves: sum of DWIA prediction with the MK transition amplitudes for $J=0$ and 1 (Table I). Dashed curves: $J=1$ calculation only.

The dashed curve corresponds to $J=1$ only and the solid curve includes the small contribution from $J=0$. Clearly, theory gives a very poor representation of both the cross sections and analyzing powers. The predicted cross sections are out of phase with the data and—on the average—much smaller. The calculated analyzing powers are also out of phase with the data.

Although the π^- data[1] for this state were described reasonably well by the MK wave functions, the predicted π^+ cross sections were much less than observed. However, the $\sigma(\pi^+)/\sigma(\pi^-)$ ratio was found to be consistent with the observed $E1$ transition rates in ^{13}C and ^{13}N (Ref. 20). Calculations for 135-MeV proton scattering[5] also failed to describe the observed cross sections for this state. Furthermore, large discrepancies were observed[21] between the form factors determined from electron scattering (both longitudinal and transverse) and theoretical predictions based on the same wave functions. These results taken together suggest quite strongly that the MK wave functions do not provide an adequate description of the $\frac{1}{2}^+$ transition. We note that, in general, theory has not been very successful[22] in describing $E1$ transitions between low-lying states. Thus a need for more theoretical work on such transitions is indicated.

3. *Transitions to the $\frac{5}{2}^+$ states at 3.85 and 6.86 MeV*

The data and DWIA curves for the first $\frac{5}{2}^+$ (3.85 MeV) state are presented in Fig. 4. The transition to this state can proceed by total angular momentum transfers to the target of $J=2$ and 3. As can be seen in Fig. 4, theory predicts significant contributions from $J=2$, orbital angular momentum transfer $L=1$, and spin transfer $S=1$ [dashed curve is the sum of $J(LS)=2(11)$ and $J=3$] at forward angles ($\lesssim 15°$), but a dominant $J=3$ transfer (dot-dash curve is $J=3$ only) at larger angles ($\gtrsim 15.0°$).

The predicted cross sections are about a factor of 2 *smaller* than the data. This factor of 2 was also found in the analysis of the scattering of 162-MeV π^+ and π^- to the same state. A deficiency in the MK densities for this transition was also indicated by the π^+/π^- cross section ratios. The pion results suggested a much larger proton contribution than predicted. The MK wave functions presumably underestimate the contributions to this transition from the collective octupole excitation of the ^{12}C core. To account for this we introduce, as was done for octupole transitions in ^{17}O in Ref. 23, an isoscalar polarization charge $\delta_0=0.51$ so that the isoscalar enhancement factor is $(1+\delta_0)=1.51$ for the $J(LS)=3(30)$ part of the transition density, resulting in good agreement between the DWIA curves and the data (Fig. 4, solid curve). If the same polarization charge is used in a calculation of the (π,π') cross sections, the agreement with the data is much improved over the MK result. Both the π^+ and π^- calculations are still smaller than the data by a factor of 0.7, but the ratio $\sigma(\pi^-)/\sigma(\pi^+)$ is much closer to that experimentally observed.

DWBA calculations for 135-MeV proton scattering[4] using spectroscopic amplitudes very similar to those of MK generated cross sections near the peak which are a factor

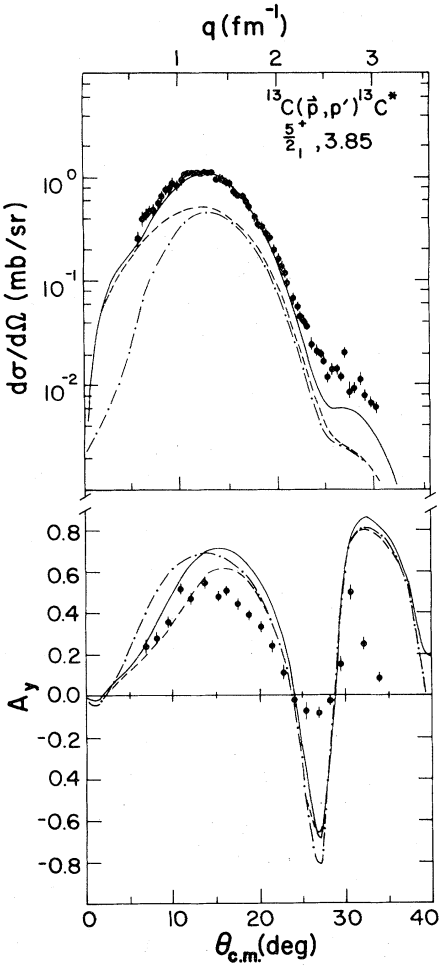

FIG. 4. $d\sigma/d\Omega_{c.m.}$ and A_y for the transition to the $\frac{5}{2}^+_1$ (3.85 MeV) state. Dot-dashed curves: DWIA predictions with the MK amplitudes for $J=3$ only. Dashed curves: sum of the predictions for $J=2$ and 3 using the MK amplitudes. Solid curves: sum of predictions for $J=2$ and 3 with the $J(LS)=3(30)$ isoscalar part of the MK amplitudes multiplied by a factor of 1.51.

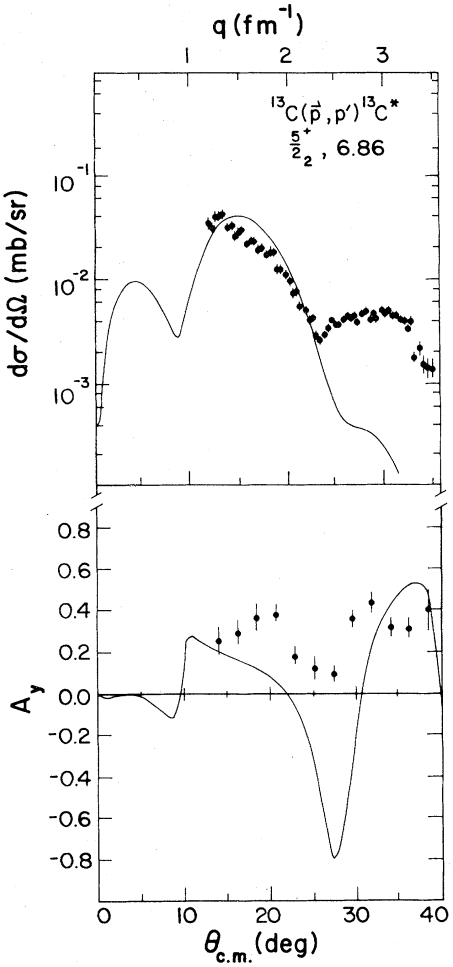

FIG. 5. $d\sigma/d\Omega_{c.m.}$ and A_y for the transition to the $\frac{5}{2}^+_2$ (6.86 MeV) state. Solid curves: DWIA predictions using the MK amplitudes.

of 2 to 3 *larger* than the data. This result from the analysis of the 135-MeV proton scattering data is inconsistent with the (π,π') work and this (p,p') study.

The components of the transition to the (weakly excited) second $\frac{5}{2}^+$ state at 6.86 MeV (Fig. 5) are predicted to be quite different from those of the first $\frac{5}{2}^+$. The latter is dominated by the $1p_{1/2}\rightarrow 1d_{5/2}$ amplitude and $J(LS)=3(30)$, the former by the $1p_{3/2}\rightarrow 2s_{1/2}$ amplitude and $J(LS)=2(11)$. The DWIA predictions for the cross sections are in reasonable agreement with the data near the second maximum, but they are much too small at $q\geq 2.5$ fm^{-1}. The $J(LS)=3(30)$ enhancement factor determined for the $\frac{5}{2}^+_1$ state was not included since it has only a very small effect on the predicted cross section. The analyzing powers do not resemble the data except for the position of the minimum near $q\simeq 2.3$ fm^{-1}. It should be noted, however, that a pure $J(LS)=3(30)$ calculation yields a cross-section shape that agrees equally well with the cross-section data and produces better agreement with the analyzing power data.

Data for this transition were not published in either the pion scattering or earlier proton scattering studies. Because the transition is extremely weak (the peak cross section is smaller than 40 μb/sr), it is possible that effects due to channel couplings are important. It is therefore not surprising to find poor agreement between the DWIA predictions and the data.

4. *Transitions to the $\frac{3}{2}^-$ (3.68 MeV) and $\frac{5}{2}^-$ (7.55 MeV) states*

The data and DWIA predictions for the collectively enhanced transitions to the lowest $\frac{3}{2}^-$ and $\frac{5}{2}^-$ states are shown in Figs. 6 and 7. The calculations give a good qualitative description of the shapes of the differential cross sections and analyzing powers for both transitions. The minima are at the correct angles, although the predicted dips in the analyzing powers are too deep. As is the case for the elastic scattering, the theoretical analyzing powers at the peaks are too large for both states.

The CK wave functions predict a significant contribu-

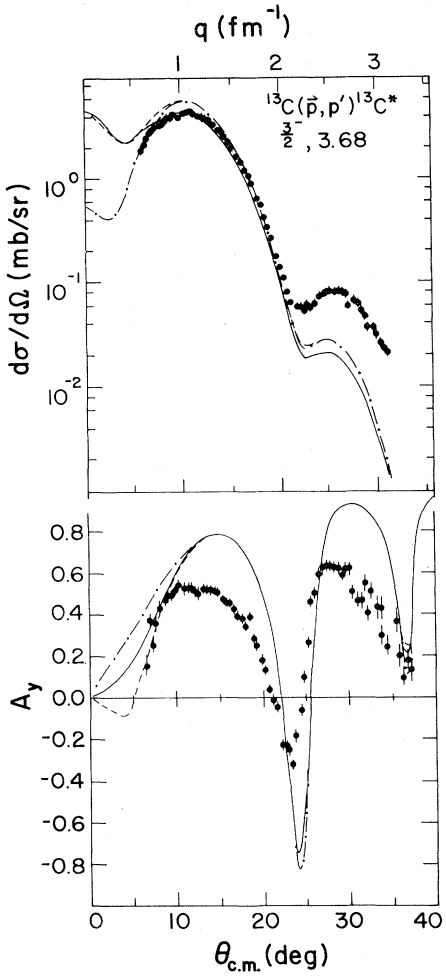

FIG. 6. $d\sigma/d\Omega_{c.m.}$ and A_y for the transition to the $\frac{3}{2}^-$ (3.68 MeV) state. Solid curves: DWIA predictions using the CK amplitudes and isoscalar and isovector enhancement factors of 1.5 and 0.46, respectively, for the $J(LS)=2(20)$ part. Dashed curves: as for the solid, but with the enhancement factors of Ref. 2. Dot-dashed curves: as for the dashed but $J=2$ only.

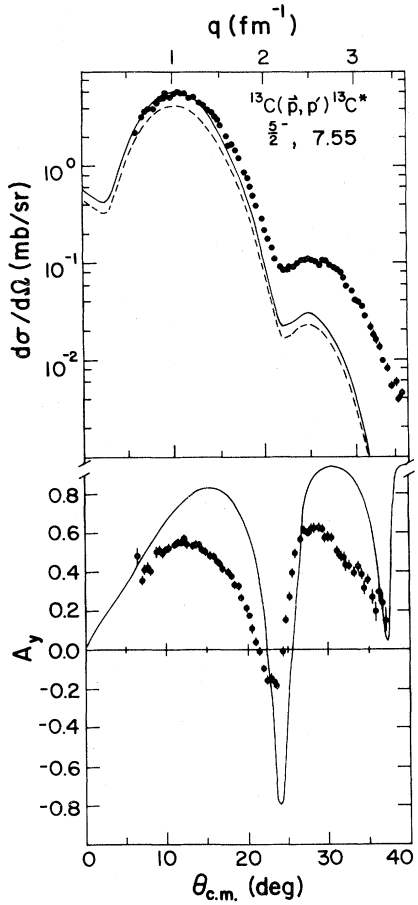

FIG. 7. $d\sigma/d\Omega_{c.m.}$ and A_y for the transition to the $\frac{5}{2}^-$ (7.55 MeV) state. Solid curves: DWIA prediction with the CK amplitudes and isoscalar and isovector enhancement factors of 1.78 and 0.77, respectively, for the $J(LS)=2(20)$ part. Dashed curves: as for the solid curves but with the enhancement factors of Ref. 2.

tion of the $J=1$ part of the transition density for the $\frac{3}{2}^-$ state at far forward angles. Although our data do not extend to small enough q to test this prediction, more recent very small angle scattering[24] has indicated a cross section for the $\frac{3}{2}^-$ state at 2.5° that is more than an order of magnitude larger than the cross section for the ^{12}C 2^+ state at 4.44 MeV.

The excitation of these states is dominated by the strong $E2$ parts of the transition densities. Lee and Kurath introduced[2] enhancement factors for the $J(LS)=2(20)$ amplitudes which reproduce known $B(E2)$ values in the p shell to predict the pion cross sections. For ^{13}C, these factors are $E_p=1.4$ for protons and $E_n=2.1$ for neutrons. DWIA calculations using these enhancements give cross sections which are somewhat too high for the $\frac{3}{2}^-$ states and too low for the $\frac{5}{2}^-$ state (dashed curves in Figs. 6 and 7).

The CK amplitudes for the $\frac{5}{2}^-$ state contain much smaller neutron than proton components. This is due to the fact that a large component of the ^{13}C(g.s.) wave function has one neutron in the $1p_{1/2}$ orbit and filled proton and neutron $1p_{3/2}$ orbits. From this piece of the ground-state wave function a $[1p_{3/2}^{-1}1p_{1/2}^{2}]_{\frac{5}{2}^-}$ state cannot be formed by a single neutron excitation. A shell-model calculation with a basis large enough to produce the correct strength for these transitions might increase the neutron contributions to the $\frac{5}{2}^-$ transition more than for the $\frac{3}{2}^-$ state. It seems that the attempt to account for the reduced basis by using common enhancement factors for both states as in Ref. 2 generates too large a neutron contribution to the $\frac{3}{2}^-$ state and does not increase the neutron contribution to the $\frac{5}{2}^-$ state enough. The need for slightly different values for E_n and E_p for the two states was also indicated by the pion analysis.

An attempt was made to improve the agreement for both states using an isoscalar effective charge $(1+\delta_0)$ to enhance the bare 2(20) amplitude. It was found that an isoscalar polarization charge $\delta_0=0.63$ for both states produces only slightly better agreement with the data than does use of the E_p and E_n enhancements of Ref. 2. The

polarization charges that are needed for the best fits are $\delta_0=0.50$ for the $\frac{3}{2}^-$ state and $\delta_0=0.78$ for the $\frac{5}{2}^-$ state. The (p,p') cross section is almost completely insensitive to changes in the isovector component of the $J(LS)=2(20)$ amplitude. Therefore, the isovector amplitude may be scaled to reproduce the observed π^+/π^- cross section ratios.[1] The result is an isovector polarization charge $\delta_1=-0.54$ for the $\frac{3}{2}^-$ state and $\delta_1=-0.28$ for the $\frac{5}{2}^-$ state. These polarization charges yield $B(E2)$ and $B(N2)$ values in good agreement with those obtained from a collective model analysis[17] of the pion scattering data. Microscopic (π,π') calculations using these effective charges are in reasonable agreement with the (π,π') data, although it seems as if the $J=1$ contribution to the $\frac{3}{2}^-$ state is overestimated in the CK transition densities.

5. *Transition to the $\frac{1}{2}^-_2$ (8.86 MeV) state*

There is strong disagreement between the DWIA predictions and the data for the $\frac{1}{2}^-_2$ state at 8.86 MeV (Fig. 8). The experimental angular distribution peaks at about $\theta_{\text{c.m.}}=10°$ ($q\simeq 0.9$ fm^{-1}) with a minimum at 20°, whereas the calculated angular distribution (solid curves) peaks at

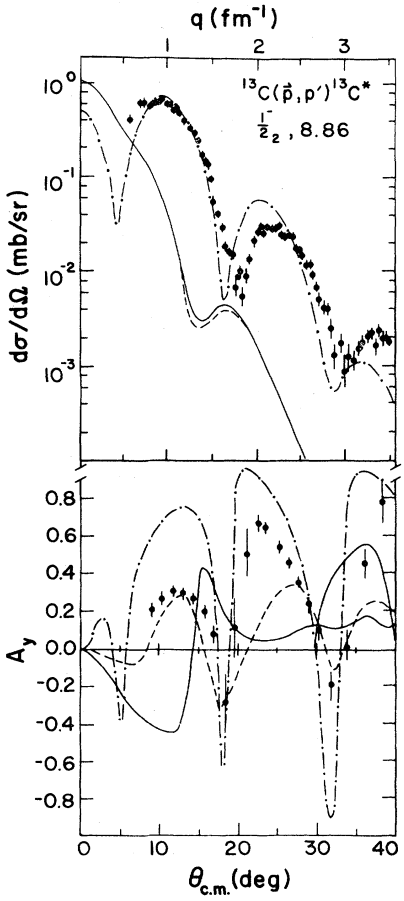

FIG. 8. $d\sigma/d\Omega_{\text{c.m.}}$ and A_y for the transition to the $\frac{1}{2}^-_2$ (8.86 MeV) state. Solid curve: DWIA prediction with the CK amplitudes. Dashed curve: as for solid curve, but with no spin-orbit optical potential. Dot-dashed curve: DWIA prediction with a pure $J(LS)=0(00)$ transition density (see the text).

0° with the first minimum at about 15°. The data and theoretical predictions for the analyzing powers are similarly out of phase. The calculations reflect the dominant $J(LS)=1(01)$, i.e., $M1$, nature of the CK transition density[3] for the first excited $\frac{1}{2}^-$ state. The CK model predicts the transition to be due to an almost pure proton excitation. The small $J=0$ ($E0$) parts of the theoretical transition density give a negligible contribution to the cross section.

To test whether the discrepancy could be explained by modifications to the spin-orbit optical potential, a calculation was done with the magnitude of the spin-orbit optical potential set equal to zero. This resulted in only a very small change in the predicted cross section and a larger change in the analyzing power (Fig. 8, dashed curve). The resulting A_y was somewhat closer to the data, but still far from a good representation of it. From this test it was concluded that it is unlikely that a reasonable modification of the spin-orbit optical potential would produce agreement with the data.

Some insight into the failure of the CK wave functions for this state can be obtained by comparing the ^{13}C data with the ^{12}C(p,p') results of Jones for the 0^+_2 (7.65 MeV) state. The data of Ref. 25 at $T_p=398$, 598, and 679 MeV, plotted as a function of q, are very similar to our data for the $\frac{1}{2}^-_2$ state in ^{13}C(8.86 MeV) at $T_p=547$ MeV, although the minima in ^{12}C occur at a slightly larger momentum transfer than in ^{13}C (1.9 vs 1.8 fm^{-1}). At $T_p=598$ MeV, the peak cross section for the 0^+_2 state in ^{12}C is about 3.6 mb/sr (Ref. 25), compared to only 0.65 mb/sr for the $\frac{1}{2}^-_2$ state in ^{13}C. Nevertheless, the similarity in the shape of the angular distributions for the two transitions suggests that the $\frac{1}{2}^-_2$ state at 8.86 MeV has a significant component of a $1p^n_{1/2}\otimes{}^{12}\text{C}(0^+)$ configuration. This conclusion was arrived at previously by Collins *et al.*[6] It has also been pointed out in Ref. 26 that the summed $E0$ strength observed in (e,e') for the $\frac{1}{2}^-_2$ (8.86 MeV) state and another $\frac{1}{2}^-$ state at 11.08 MeV is nearly equal to the $E0$ strength for the $^{12}\text{C}(0^+_1\rightarrow 0^+_2)$. We note that the 0^+_2 state in ^{12}C is not contained in the $1p$ shell model of Cohen and Kurath.

In order to compare the predictions of the CK transition densities with a pure $J(LS)=0(00)$ density, which would be appropriate to an $E0$ transition such as the $0^+_1\rightarrow 0^+_2$ in ^{12}C, we used the appropriate combination of isoscalar $1p_{1/2}\rightarrow 2p_{1/2}$ and $1p_{3/2}\rightarrow 2p_{3/2}$ components with $b=1.67$ fm (the same harmonic oscillator parameter as for all calculations here). The shape of the predicted differential cross sections using this density is in much improved agreement with the data (Fig. 8 dot-dashed curve), and the analyzing powers are in phase with the measured A_y, in contrast to the predictions using the CK densities. The difference in phase between the two predictions is primarily due to the use of pure 0(00) versus the mixed 1(01)/1(21) transition density of Ref. 2. The change in the radial dependence of the densities (pure $1p$ shell vs $1p\rightarrow 2p$ shell) has only a minor effect. The fit to the data is not perfect, e.g., the relative cross section at the third maximum ($q\simeq 2$ fm^{-1}) is too large in the calculation, but this is not unreasonable considering the artificial nature of the transition density. The first maximum in

the predicted A_y is much larger than the data, similar to the discrepancy in the elastic analyzing powers.

The analysis of the pion data[3] for this state also revealed severe discrepancies between theoretical predictions[2] and experiment.[1] The theoretical transition density is dominated by a pure proton, $M1$, excitation. The cross section ratio $\sigma(\pi^+)/\sigma(\pi^-)$, however, showed that the transition is not a pure proton excitation. Furthermore, as for the (p,p') case, the (π,π') calculations with the CK densities do not reproduce the shape nor the magnitude of the differential cross sections. We therefore conclude that the $\frac{1}{2}^-_2$ state at 8.86 MeV excitation is not the $\frac{1}{2}^-$ state of the $1p$-shell model of Cohen and Kurath. Rather, the proton and pion data suggest, in agreement with Ref. 6, that this state has a large component of a $1p_{1/2}$ neutron coupled to the first excited 0^+ state in ^{12}C(7.66 MeV).

6. *Transition to the $\frac{9}{2}^+$ (9.5 MeV) state*

The data and DWIA predictions for the transition to the $\frac{9}{2}^+$ "stretched" state at 9.5 MeV are shown in Fig. 9. The MK transition density for this state consists of essentially a pure neutron $1p_{3/2}\rightarrow 1d_{5/2}$ component. In our calculations we have not included the very small proton component (see Table II). The $1p_{3/2}\rightarrow 1d_{5/2}$ one-particle–one-hole excitation is the only one that can make a spin of $\frac{9}{2}^+$ in a $1\hbar\omega$ basis. Such an excitation proceeds by $J(LS)=4(31)$ only.

The calculations reproduce the shapes of the differential cross sections and analyzing powers quite well. The experimentally observed shoulder on the angular distribution at $q\geq 3.2$ fm^{-1}, however, is not described. The magnitude of A_y is underestimated at small q and, as for most other transitions observed here, the predicted minimum is too deep.

The DWIA cross sections using the MK transition densities[4] for the excitation of the $\frac{9}{2}^+$ state were multiplied by a factor of $R=0.43$ to reproduce the magnitude of the experimental cross sections. This value is smaller than the value $R=0.65$ deduced in Ref. 1 from the pion scattering. However, newer (π,π') calculations with an improved optical potential require a renormalization consistent with that determined here. Since we deal here with a pure $M4$ transition, quenching of the shell model strength by a factor of about 0.4 is not unexpected. This result is in disagreement with some of the conclusions drawn from the analysis[5,6] of 135-MeV proton scattering to the $\frac{9}{2}^+$ state. There, the transition density was obtained from a shell model calculation which is similar to that of MK but yielded a slightly smaller fraction of the single particle strength. The resulting prediction for $\sigma(\theta)$ in Ref. 5 was about 20% *smaller* than the data so that $R=1.2$. However, in Ref. 6 a larger $\sigma(\theta)$ and thus $R=0.7$ was predicted with a different parametrization of a free NN interaction.

The 547- and 135-MeV data for the $\frac{9}{2}^+$ state have the common feature of a shoulder on the large q side of the angular distributions ($q\simeq 3.2$ fm^{-1}). The DWIA predictions (when normalized at the peak) are much too small at these large momentum transfers for both energies. Since the transition densities used here involve only $1\hbar\omega$ excitations, the failure to reproduce the large-q data may indicate the need for $3\hbar\omega$ or higher terms in the transition density.

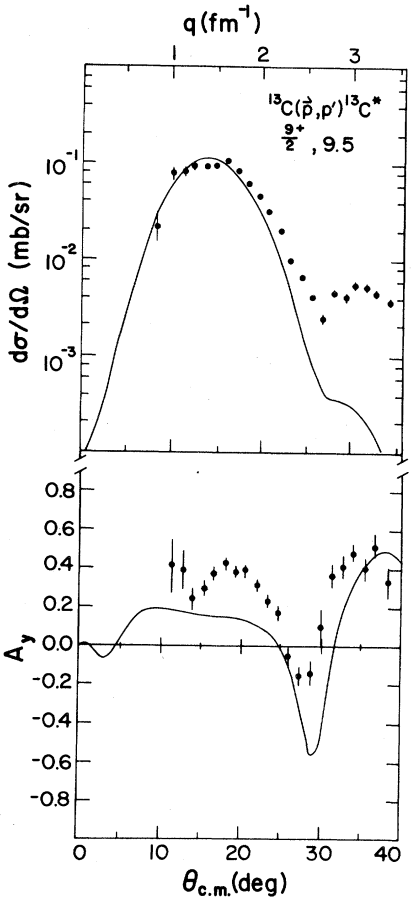

FIG. 9. $d\sigma/d\Omega_{c.m.}$ and A_y for the transition to the $\frac{9}{2}^+$ (9.5 MeV) state. Solid curve: DWIA predictions with the MK amplitude and scaled by a factor of 0.43.

IV. CONCLUSIONS

The elastic scattering cross sections and analyzing powers calculated by folding ground state densities with a NN interaction are in very good agreement with the data. In particular, the deep forward-angle dip in $A_y(\theta)$ is reproduced by the IA calculations. This is in contrast to the results for ^{40}Ca and ^{208}Pb where relativistic Dirac calculations[27] are necessary to reproduce this feature of the $A_y(\theta)$ data. For ^{16}O, where the nonrelativistic calculations provide a qualitative description of the $A_y(\theta)$ data, the relativistic Dirac calculations make a smaller improvement, in particular a decrease in the magnitude of $A_y(\theta)$ near the first maximum. A similar effect would also improve agreement for ^{13}C. Such calculations have not been done for ^{13}C, where it would be interesting to see if the additional spin components for this odd-A nucleus would be important.

Calculations of pion elastic scattering using the same ground state densities as used in our IA calculations gave

equally good agreement[17] with the pion data. This supports the concept that the impulse approximation for the π-N and N-N interactions used here is valid.

The shell model wave functions of Refs. 3 and 4 provide a reasonable description of inelastic proton scattering at $T_p = 547$ MeV for the transitions to the $\frac{9}{2}^+$, $\frac{5}{2}^+_1$, $\frac{3}{2}^-$, and $\frac{5}{2}^-$ states in ^{13}C when scaling factors which are consistent with $B(E\lambda)$ values and pion scattering analyses are used. The wave functions for the $\frac{1}{2}^+$ and $\frac{1}{2}^-_2$ states, however, fail completely in predicting the shapes of the differential cross sections and analyzing powers. These failures were also found in the analysis of 162 MeV pion scattering and 135 MeV proton scattering for the same states.

In summary, the consistent results obtained for pion and proton scattering for four states in ^{13}C indicate that the reaction models are adequately understood. Thus the disagreements between experiment and theory for the $\frac{1}{2}^-_2$ and $\frac{1}{2}^+$ transitions show insufficiencies in the nuclear structure calculations. The problems associated with the $\frac{1}{2}^+$ state may be part of the general theoretical difficulties in describing $E1$ transitions between low-lying states. The $\frac{1}{2}^-_2$ state appears to be a state not contained in the $1p$-shell model of Ref. 3.

We thank Dr. B. M. Spicer for helpful comments and Dr. S. F. Collins for pointing out an error in our original calculations.

---

*Present address: Los Alamos National Laboratory, Los Alamos, NM 87545.

[1]S. J. Seestrom-Morris *et al.*, Phys. Rev. C **26**, 594 (1982).
[2]T.-S. H. Lee and D. Kurath, Phys. Rev. C **21**, 293 (1980); **22**, 1670 (1980).
[3]S. Cohen and D. Kurath, Nucl. Phys. **73**, 1 (1965).
[4]D. J. Millener and D. Kurath, Nucl. Phys. **A255**, 315 (1975).
[5]L. Rikus *et al.*, Aust. J. Phys. **35**, 9 (1982).
[6]S. F. Collins *et al.*, Nucl. Phys. **A380**, 445 (1982).
[7]G. S. Blanpied, Ph.D. dissertation, University of Texas, 1977; Los Alamos National Laboratory Report LA-7262-T, 1978.
[8]G. S. Blanpied *et al.*, Phys. Rev. C **18**, 1436 (1978).
[9]W. G. Love and M. A. Franey, based on the SM82 amplitudes of R. A. Arndt and L. D. Roper (unpublished).
[10]W. G. Love and M. A. Franey, Phys. Rev. C **24**, 1073 (1981).
[11]G. W. Hoffmann *et al.*, Phys. Rev. C **21**, 1488 (1980).
[12]R. A. Arndt, nucleon-nucleon scattering amplitudes set WI82 (private communication).
[13]M. Outhoudt, computer code PEKFIT (unpublished).
[14]L. E. Smith, computer code LOAF (unpublished).
[15]R. Schaeffer and J. Raynal, computer code DWBA70 (unpublished).
[16]J. Carr, F. Petrovich, and J. Kelly, computer program ALLWORLD (unpublished).
[17]S. J. Seestrom-Morris *et al.*, Phys. Rev. C **28**, 1301 (1983).
[18]G. W. Hoffman *et al.*, Phys. Rev. C **27**, 1436 (1981).
[19]M. V. Hynes *et al.*, Phys. Rev. Lett. **52**, 978 (1984).
[20]P. Endt, At. Data Nucl. Data Tables **23**, 3 (1979).
[21]R. S. Hicks (private communication).
[22]P. J. Ellis (private communication).
[23]C. L. Blilie *et al.*, submitted to Phys. Rev. C.
[24]J. B. McClelland (private communication).
[25]K. W. Jones, Ph.D. thesis, Rutgers State University, 1982.
[26]G. Wittwer, H.-G. Clerc, and G. A. Beer, Phys. Lett. **30B**, 634 (1969).
[27]B. C. Clark *et al.*, Phys. Rev. Lett. **50**, 1644 (1983).